LONG VALLEY OBSERVATORY QUARTERLY REPORTS
COMBINED July – December 2008

Long Valley Observatory
U.S. Geological Survey
Volcano Hazards Program, MS 910
345 Middlefield Rd., Menlo Park, CA 94025

http://lvo.wr.usgs.gov

This report is a preliminary description of unrest in Long Valley caldera and Mono-Inyo Craters region of eastern California. Information contained in this report should be regarded as preliminary and is not be cited for publication without approval by the Scientist in Charge of the Long Valley Observatory. The views and conclusions contained in this document do not necessarily represent the official policies, either express or implied, of the U.S. Government.

LONG VALLEY OBSERVATORY QUARTERLY REPORTS
July – December 2008

CONTENTS

SUMMARY FOR JULY – DECEMBER 2008

The relative quiescence in Long Valley caldera that began in the spring of 1998 continued through 2008. Earthquake activity within the caldera remained low with slightly elevated activity beneath Mammoth Mountain. The latter included a number of small swarms and spasmodic bursts with a M=2.5 earthquake during a swarm on October 15. The largest regional earthquake was a M=3.2 event near Big McGee Lake in the Sierra Nevada on July 10. The resurgent dome, which essentially stopped inflating in early 1998 and showed minor subsidence (of about 1 cm) through 2001, was followed by gradual inflation through 2002. The deformation pattern since 2003 has been characterized by gradual subsidence that appears to have flattened out in early 2007. The center of the resurgent dome remains some 75 cm higher than prior to the onset of unrest in 1980. Carbon dioxide emissions around Mammoth Mountain continue to fluctuate with measurement in the Horseshoe Lake area varying between 50 and 100 tons/day. Repeat measurements of CO_2 flux sites on the Mono Craters shows that the North Coulee continues to produce about 9 tons/day with an isotopic composition essentially the same as that for Mammoth Mountain.

Up-to-date plots for most of the data summarized here are available on the Long Valley Observatory web pages (http://lvo.wr.usgs.gov).

EARTHQUAKES *(D.P. Hill and A.M. Pitt)*

LONG VALLEY CALDERA AND MAMMOTH MOUNTAIN ACTIVITY:
Low levels of earthquake activity beneath Long Valley caldera continued through the last six months of 2008. None of the earthquakes within the caldera during this period exceeded magnitude M=2.0. Mammoth Mountain activity increased somewhat with swarms of small earthquakes on July 15, August 10, October 15, and December 14. Each of these swarms included one or more "spasmodic bursts", or rapid-fire sequences of small, earthquakes with overlapping seismic waves commonly with durations of several minutes. The largest of the Mammoth Mountain earthquakes was a M = 2.5 event during the October 15 swarm.

SIERRA NEVADA ACTIVITY
As has been true since 1999, earthquake activity in the Sierra Nevada block south of the caldera continues at a higher rate than beneath either the caldera or Mammoth Mountain with most of the activity concentrated in a band extending from the southern margin of the caldera for some 20 km to the south-southwest (Figures S1-S7). The two largest earthquakes in the region during the second half of 2008 included a M=3.2 event on July 10 near Big McGee Lake and a M=3.1 event on August 19 located beneath Pine Creek canyon 1 mile north of Scheelite.

REGIONAL ACTIVITY
Elsewhere in the region, earthquake activity at the magnitude 2 level was scattered in a diffuse zone between Round Valley and Bishop, in the Chalfant Valley area, and in the Adobe Hills just east of Mono Lake.

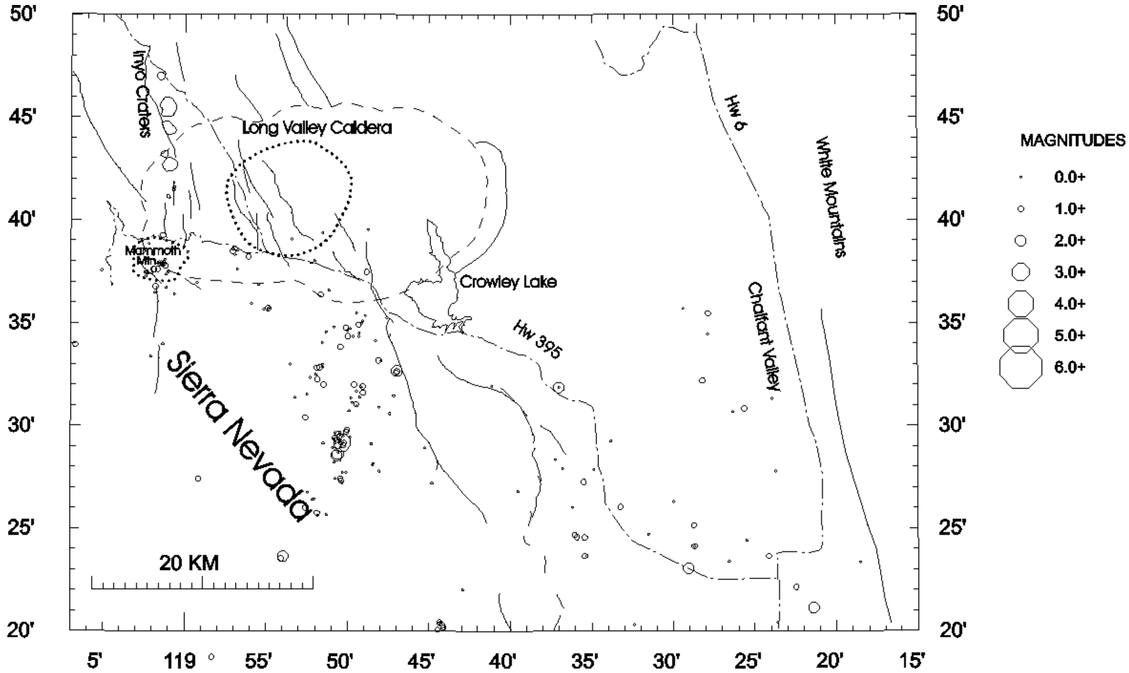

Figure S1: Earthquake epicenters (ALL) in the Long Valley region for Jul. 2008

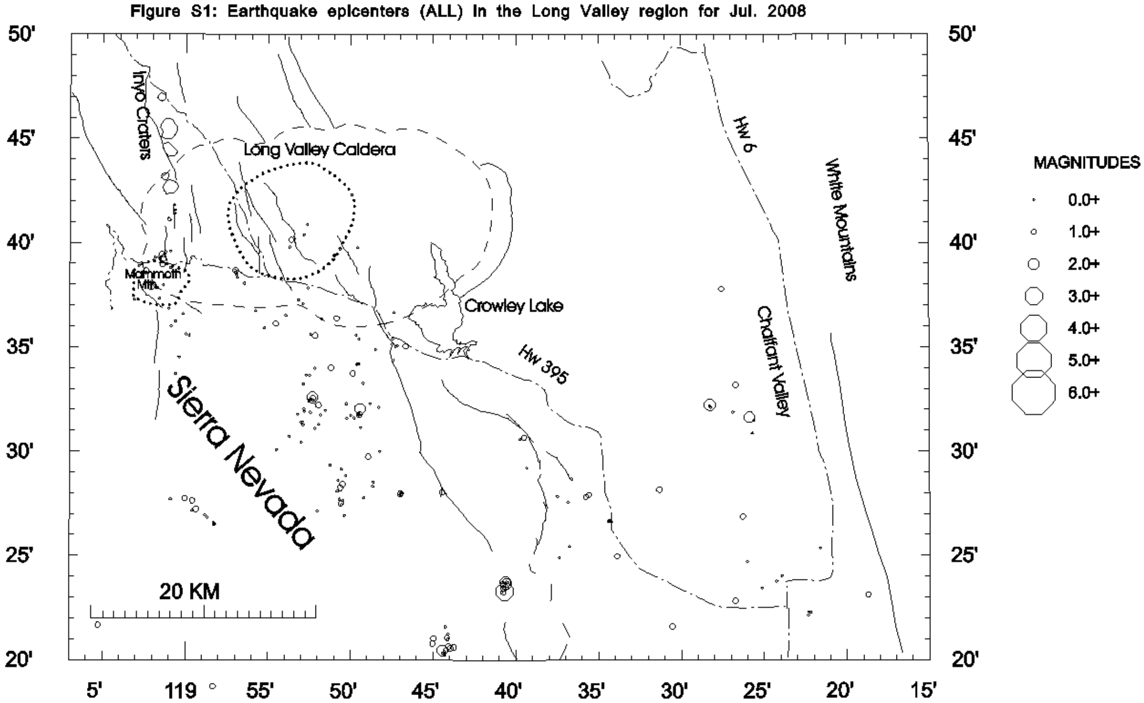

Figure S2: Earthquake epicenters (ALL) in the Long Valley region for Aug. 2008

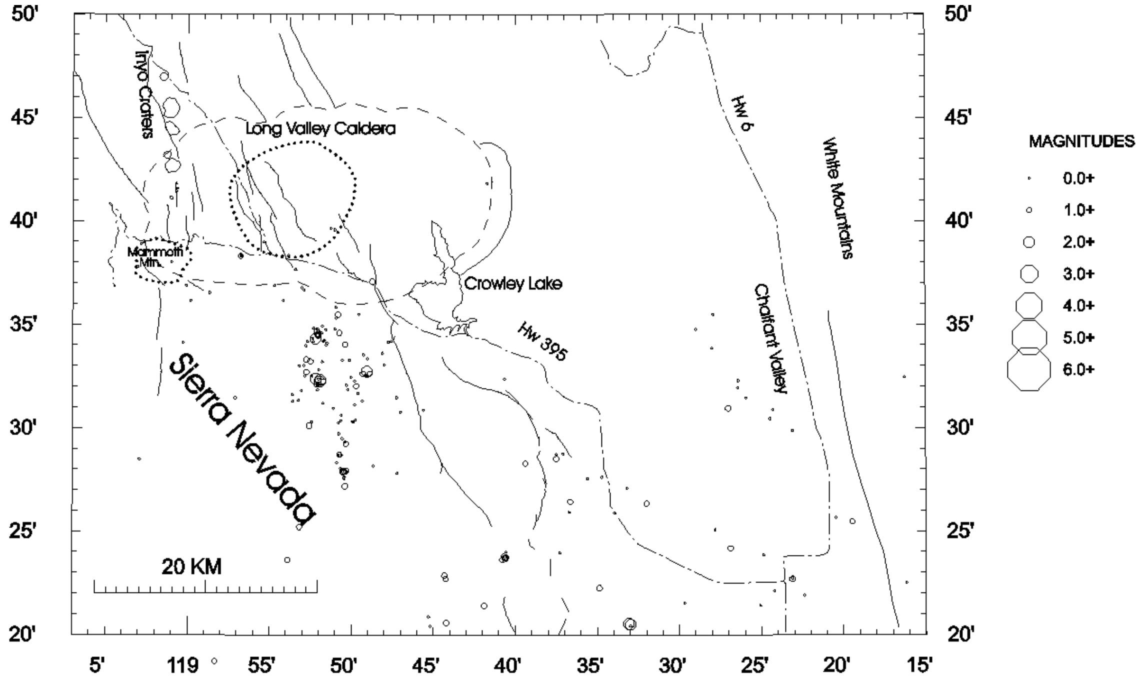

Figure S3: Earthquake epicenters (ALL) in the Long Valley region for Sep. 2008

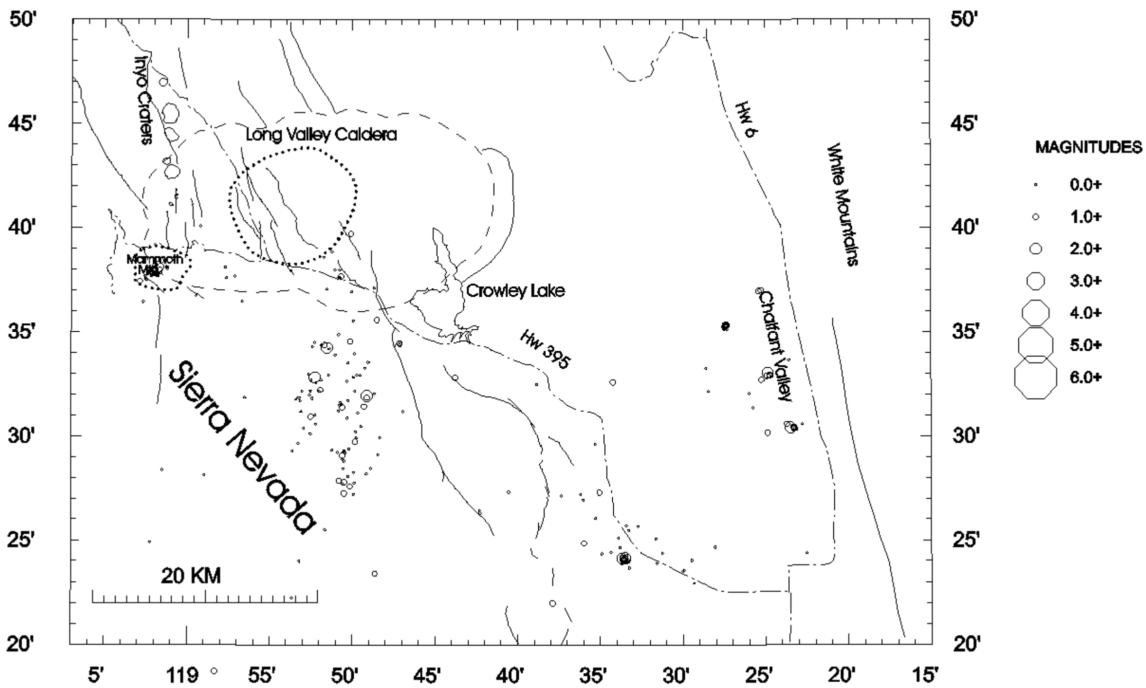

Figure S4: Earthquake epicenters (ALL) in the Long Valley region for Oct. 2008

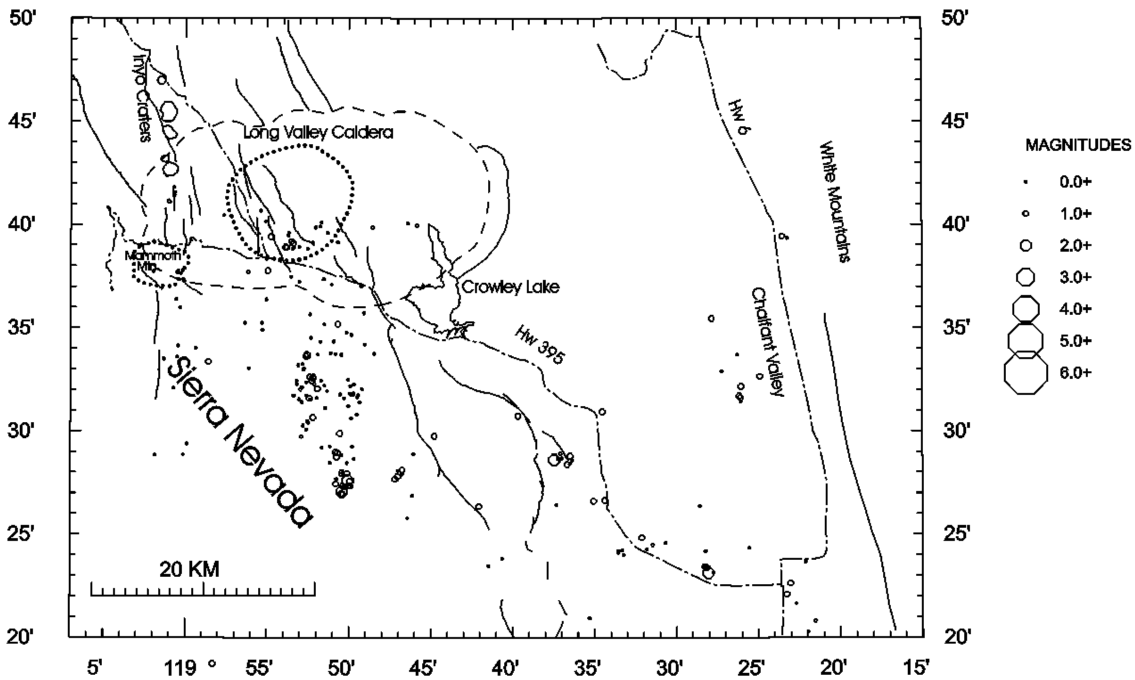

Figure S5: Earthquake epicenters (ALL) in the Long Valley region for Nov. 2008

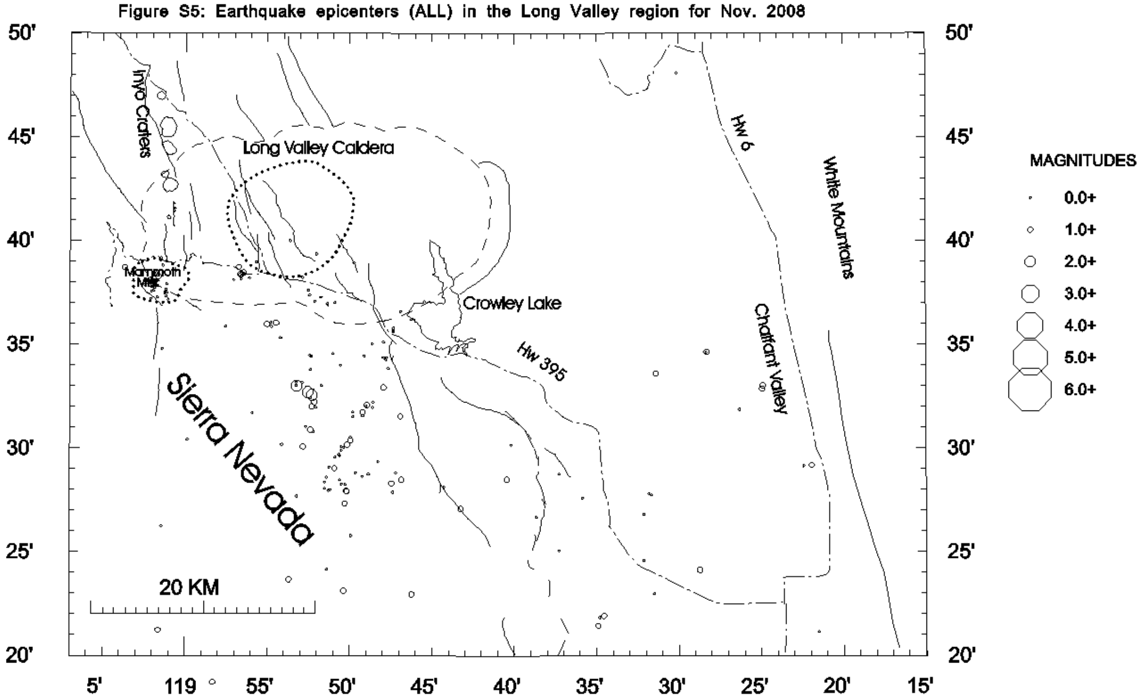

Figure S6: Earthquake epicenters (ALL) in the Long Valley region for Dec. 2008

DEFORMATION

SUMMARY OF EDM AND GPS MEASUREMENTS

John Langbein, Stuart Wilkinson, Mike Lisowski, Eugene Iwatsubo, and Jerry Svarc

Over the past 8 years, 18 GPS (Global Position System) receivers have been installed within and near the Long Valley Caldera. Of these, 14 were installed by Elliot Endo of the Cascades Volcano Observatory. The locations of the 12 receivers within the caldera are shown in Figure G1. The close correlation of variations in baseline lengths between the EDM measurements that began in 1984 and the GPS measurements, the first of which began in 1999 (Figures G1, G2, G3), has allowed us to discontinue the expensive, labor-intensive EDM measurement in October of 2006. In the future, we will rely entirely on the GPS measurements.

Recent results from the GPS data indicate that the gradual shortening of the baseline lengths by 1 to 3 cm from 2004 through 2006 (consistent with subsidence of the resurgent dome by a comparable amount) reversed trend through mid 2007 and has shown slow extension over the past six months (Figures G2, G3). Over the long term, the center of the resurgent dome remains some 75 cm higher than prior to the onset of caldera unrest in 1980 (see http://lvo.wr.usgs.gov/monitoring/index.html#deformation)

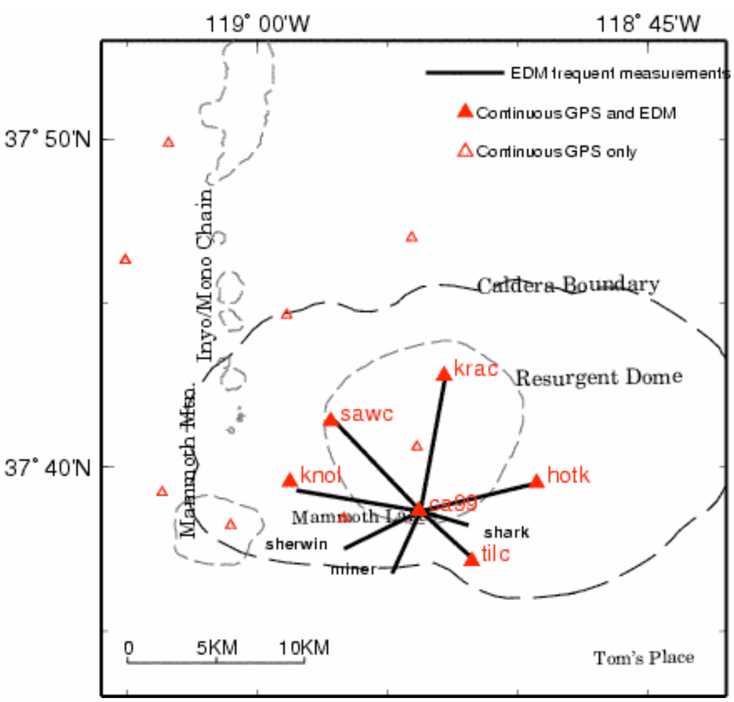

Figure G-1 Map showing 2-color EDM baselines

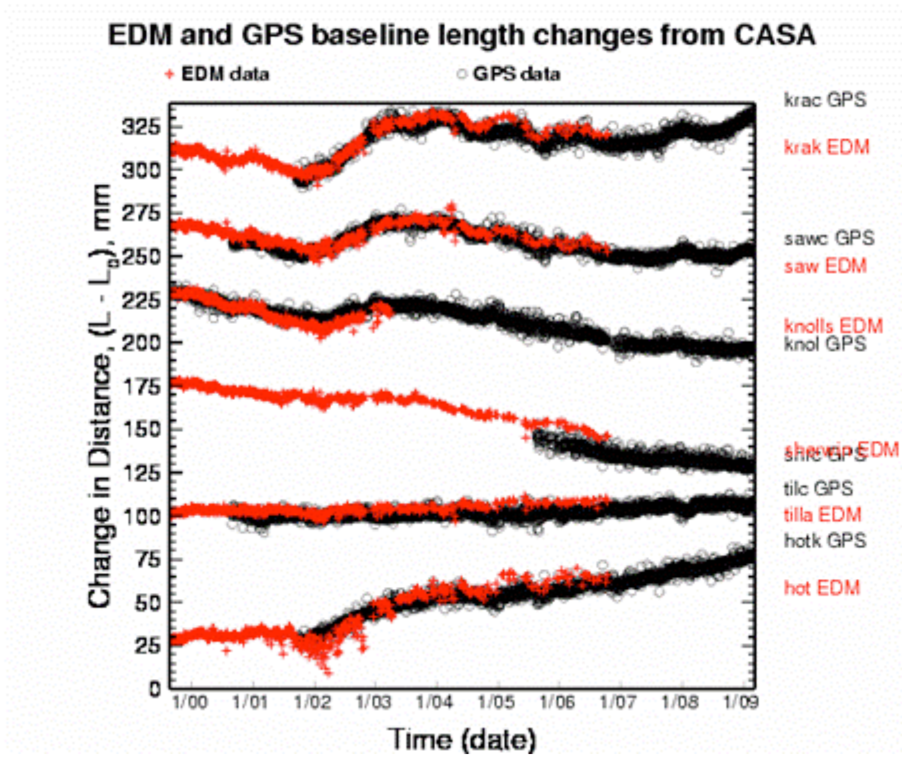

Figure G2.Line-length changes for the EDM baselines (red crosses) measured from CASA for the period February 12, 1999 through October 3 2007 compared with continuous GPS data for the same lines (black circles). Note that the EDM measurements were discontinued in October 2006.

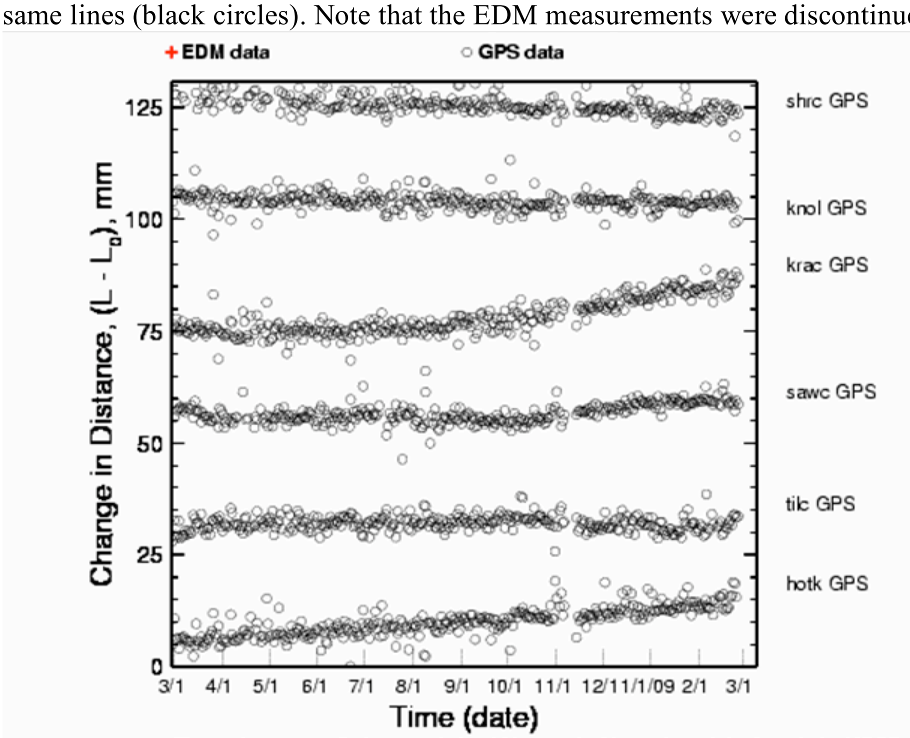

Figure G3. Line-length changes for the continuous GPS baselines spanning the resurgent dome from March 2008 through the end of February 2009.

CONTINUOUS BOREHOLE STRAIN MEASUREMENTS (Malcolm Johnston, Doug Myren, and Stan Silverman)

Instrumentation

Dilational strain measurements are being recorded continuously at the Devil's Postpile (POP), Motorcross (MX) near the western moat boundary in the south moat, Big Springs (BS) just outside the norhtern caldera boundary, and at Phillips (PLV1), just to the north of the town of Mammoth Lakes. The site locations are shown in Figure D1. The instruments are Sacks-Evertson dilational strain meters and consist of stainless steel cylinders filled with silicon oil that are cemented in the ground at a depth of about 200m. Changes in volumetric strain in the ground are translated into displacement and voltage by a expansion bellows attached to a linear voltage displacement transducer. This instrument is described in detail by Sacks et al.(*Papers Meteol. Geophys*. ,22, 195, 1971).

Data from the strainmeters are transmitted using satellite telemetry every 10 minutes to a host computer in Menlo Park. The data are also transmitted with 24-bit seismic telemetry together with 3-component seismic data to Menlo Park.

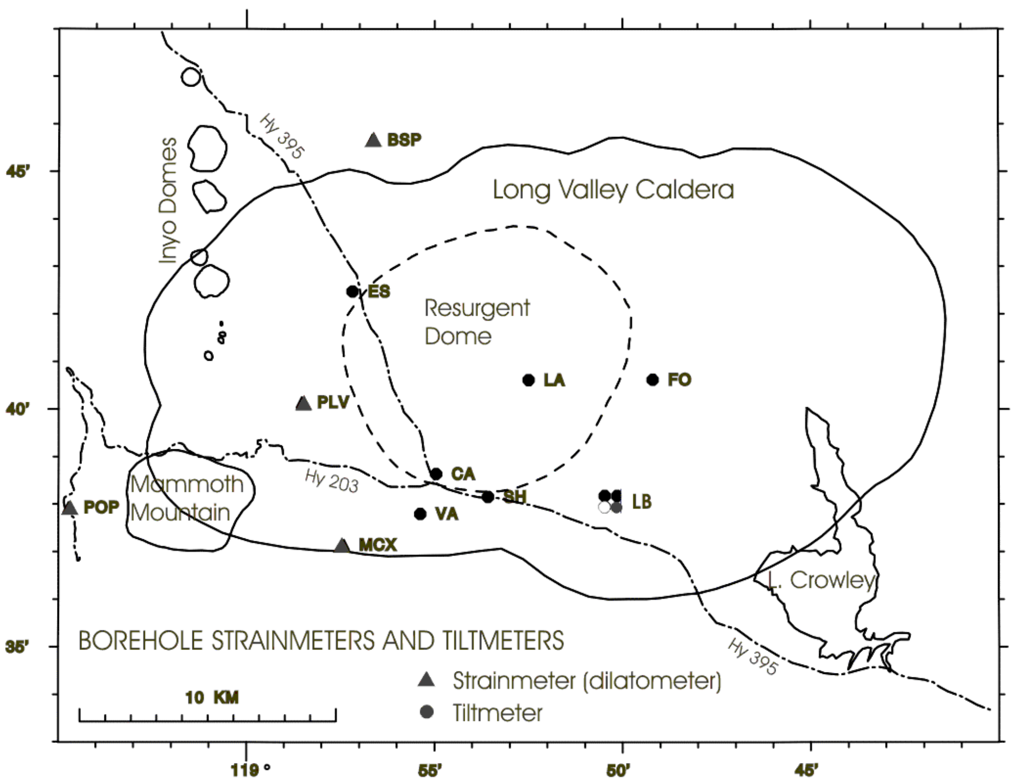

.
Figure D1. Locations of dilatometers and tiltmeters.

Highlights

The data during this quarter has been relatively quiet at all sites.

Pressure corrected data are shown in Figures S2 and S3. Comparative pore pressure at the Postpile dilatometer site and at the Big Springs site is shown in Figure S4. Postpile continues to show gradual decrease in compression compared to the 1990's. The long term record is shown in S5.

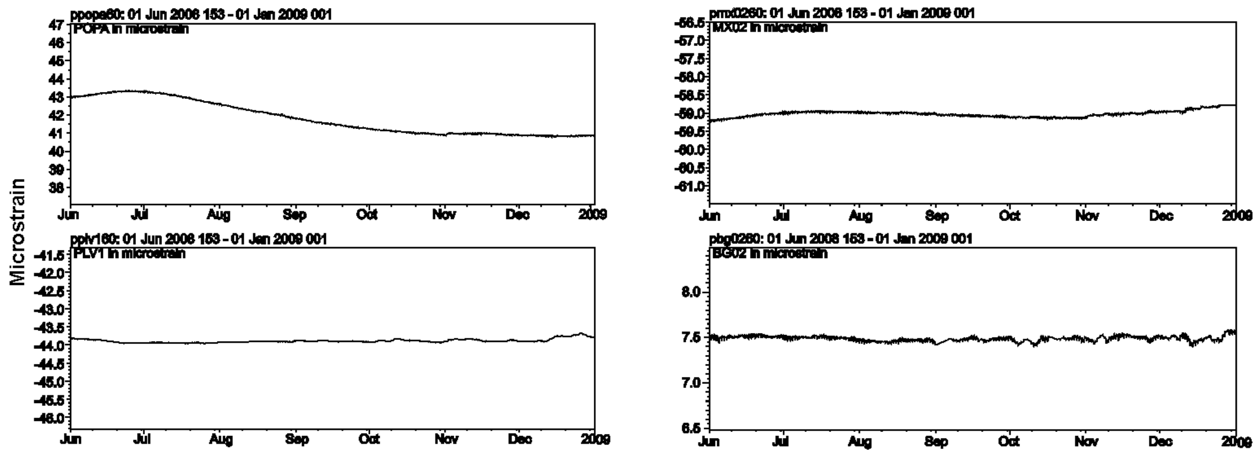

Figure D2. Dilational strain for POPA, PLV1, MX, and BG bore-hole dilatometers for June-December 2008

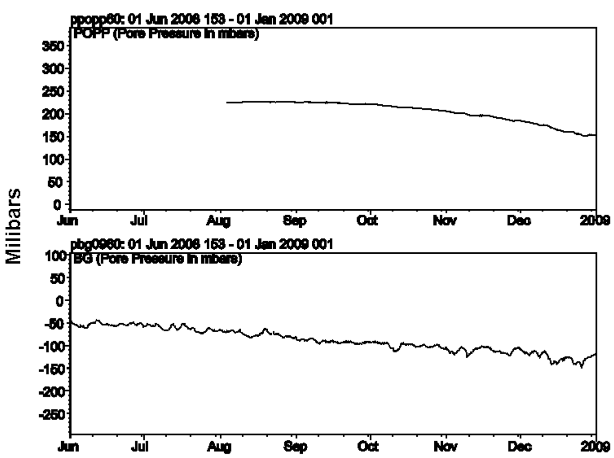

Figure D3. Pore pressure for POPA and BG bore-hole dilatometer sites for June-December 2008

TILT MEASUREMENTS (Mal Johnston, Roger Bilham, Doug Myren and Stuart Wilkensen)

Instrumentation

Instruments recording crustal tilt in the Long Valley caldera are of two types - 1) a long-base (LB) instrument in which fluid level is measured in fluid reservoirs separated by about 500 m and connected by pipes, which was constructed by Roger Bilham of the University of Colorado, and 2) borehole tiltmeters that measure the position of a bubble trapped under a concave lens. For tiltmeter locations, see Figure D1. Real time plots of the data from these instruments can be viewed at http://quake.wr.usgs.gov/QUAKE/longv.html.

All data are transmitted by satellite to the USGS headquarters in Menlo Park, CA Data samples are taken every 10 minutes. Plots of the changes in tilt as recorded on each of these tiltmeters are shown in Figures T1-T3. Removal of re-zeros, offsets, problems with telemetry and identification of instrument failures is difficult, tedious and time-consuming task. In order to have a relatively up-to-date file of data computer algorithms have been written that accomplish most of these tasks most of the time. Detailed discussion or detailed analysis usually requires hand checking of the data. Flat sections in the data usually denote a failure in the telemetry. Gaps denote missing data. All instruments are scaled using tidally generated scale factors.

Highlights

Fig T1 shows the long base data from June 1, 2008 to Jan 1, 2009. Data from the tiltmeters in the deep boreholes at Big Springs and Motorcross are shown in T2 .No changes of note are apparent. Data from the short base tiltmeters are shown in Figures T3. Very little of geophysical interest occurred this period.

.

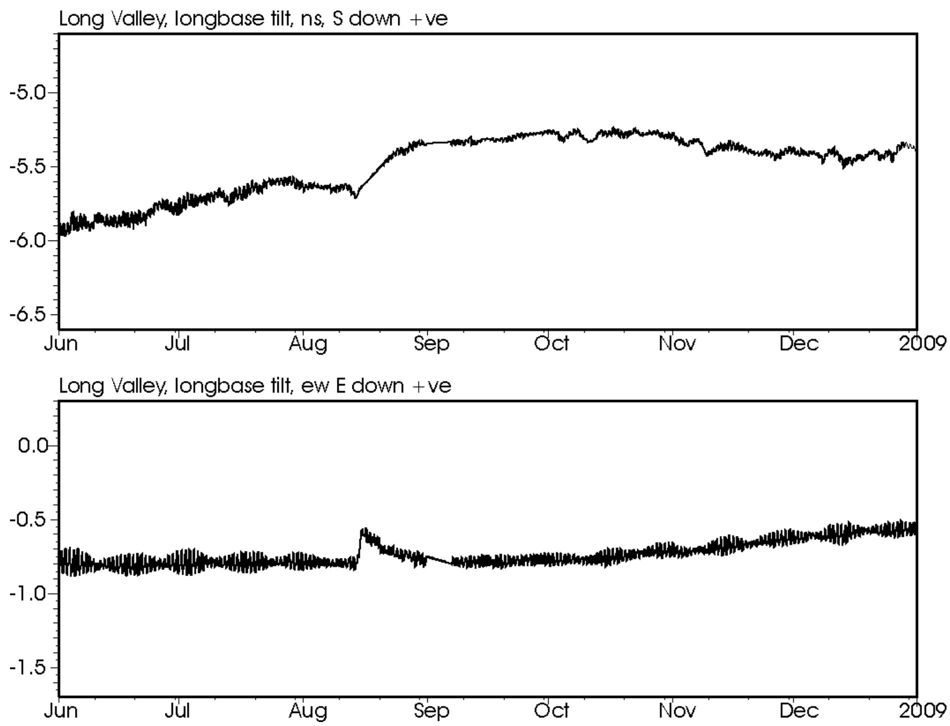

Figure T1. East-west and north-south components of the long-base tiltmeter for 1 June through December 2008. Positive slopes indicate tilt down the south and east, respectively. Units in microradians.

.

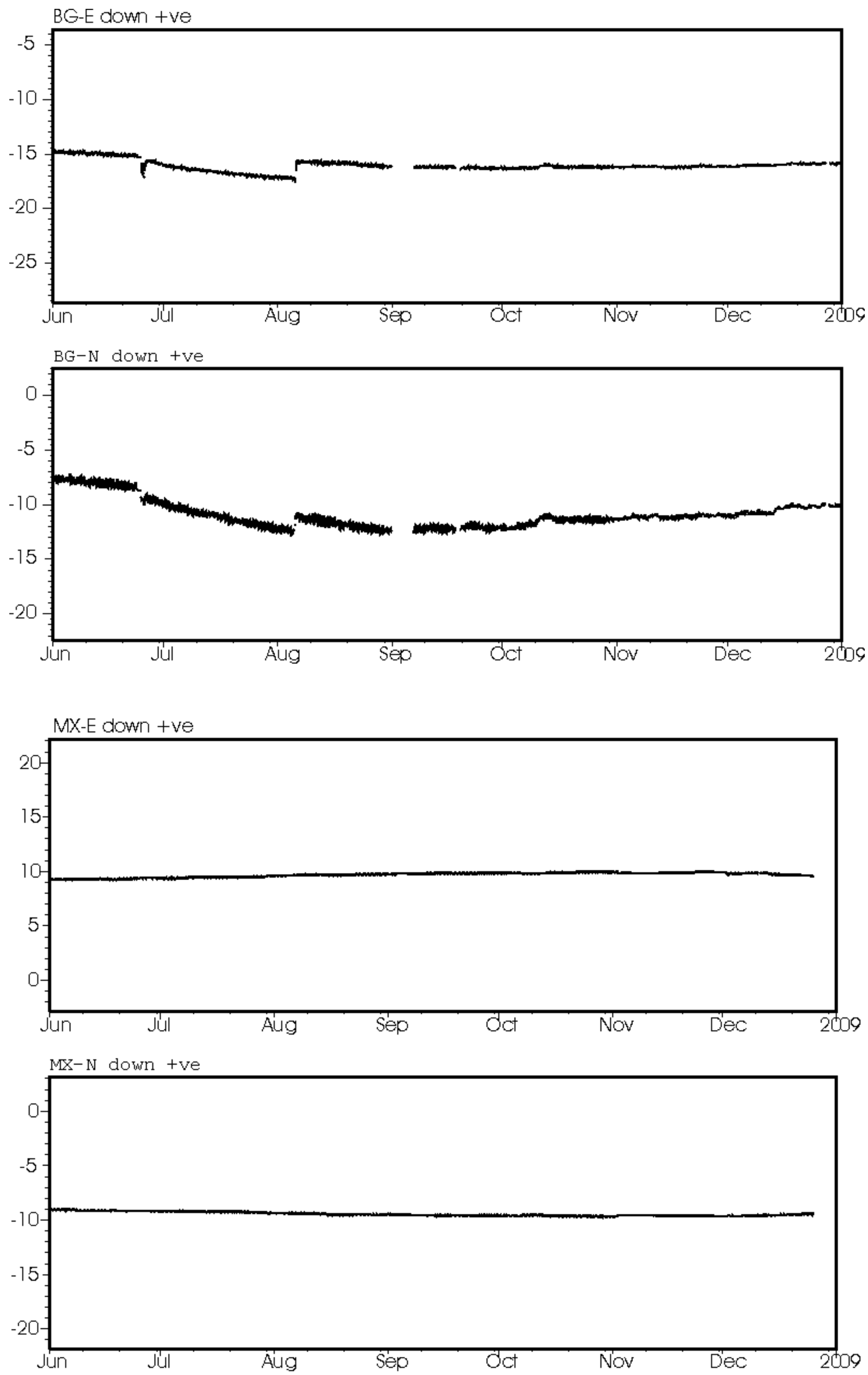

Figure T2. East-west and north-south components for the borehole tiltmeters installed with the Big Springs (BS) and Motocross (MX) dilatometers for June – December 2008. Units in microradians.

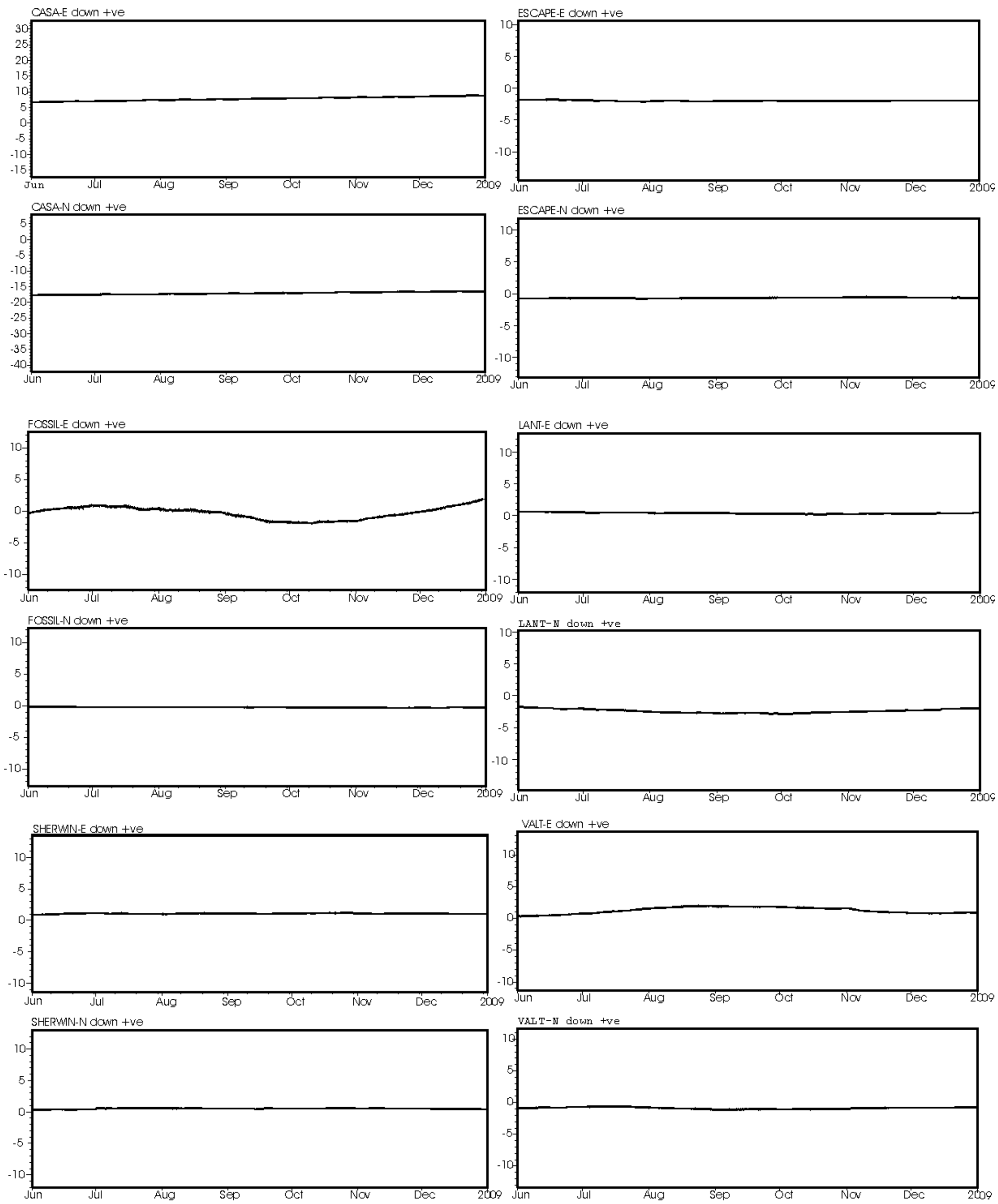

Figure T3. East-west and north-south tilt components for the shallow borehole tiltmeters for June-December 2008. Units in microradians.

MAGNETIC MEASUREMENTS (M.J.S. Johnston, S. Wilkinson, Doug Myren, Y. Sassai, and Y. Tanaka)

Background

Local magnetic fields at 18 sites in the Long Valley Caldera are transmitted via satellite telemetry to Menlo Park every 10 minutes. These and other data provide continuous 'real-time' monitoring in this region through the low-frequency data system. The location of these sites is shown on Figure M1. Temporal changes in local magnetic field are isolated using simple differencing techniques.

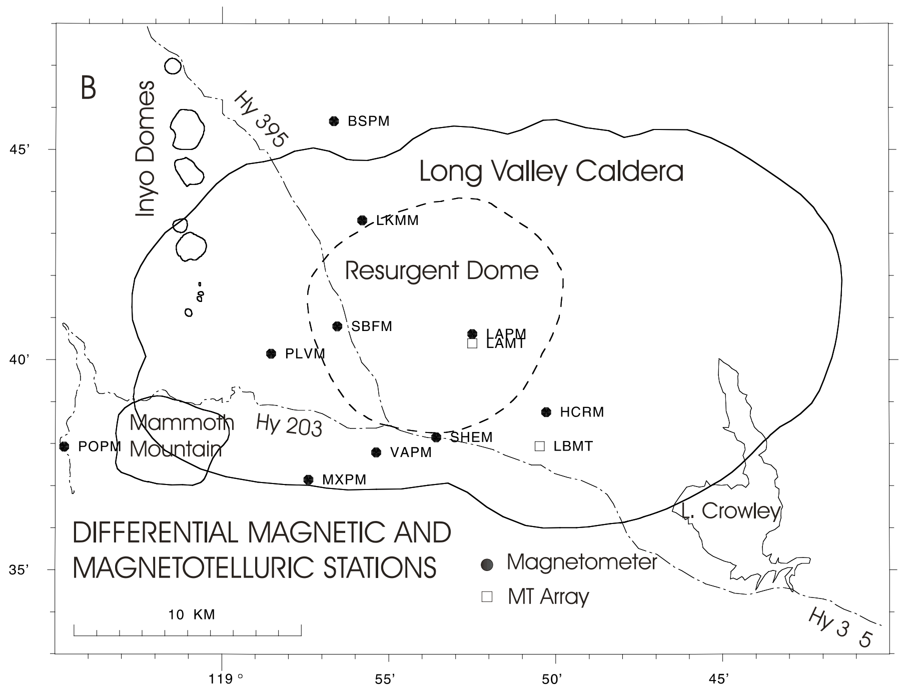

Figure M1. Locations of differential magnetic field stations within Long Valley caldera. The reference station MGS (not shown) is located along Highway 395 approximately 20 km southeast of the caldera.

Data:
Plots of daily averaged data from the telemetered magnetometer stations in and near the caldera are shown in Figures M2.. As these instrument are getting old we are having great difficulty keeping them alive. Dedicated work by Stuart Wilkinson is greatly appreciated.

Highlights:
Nothing unusual during this quarter.

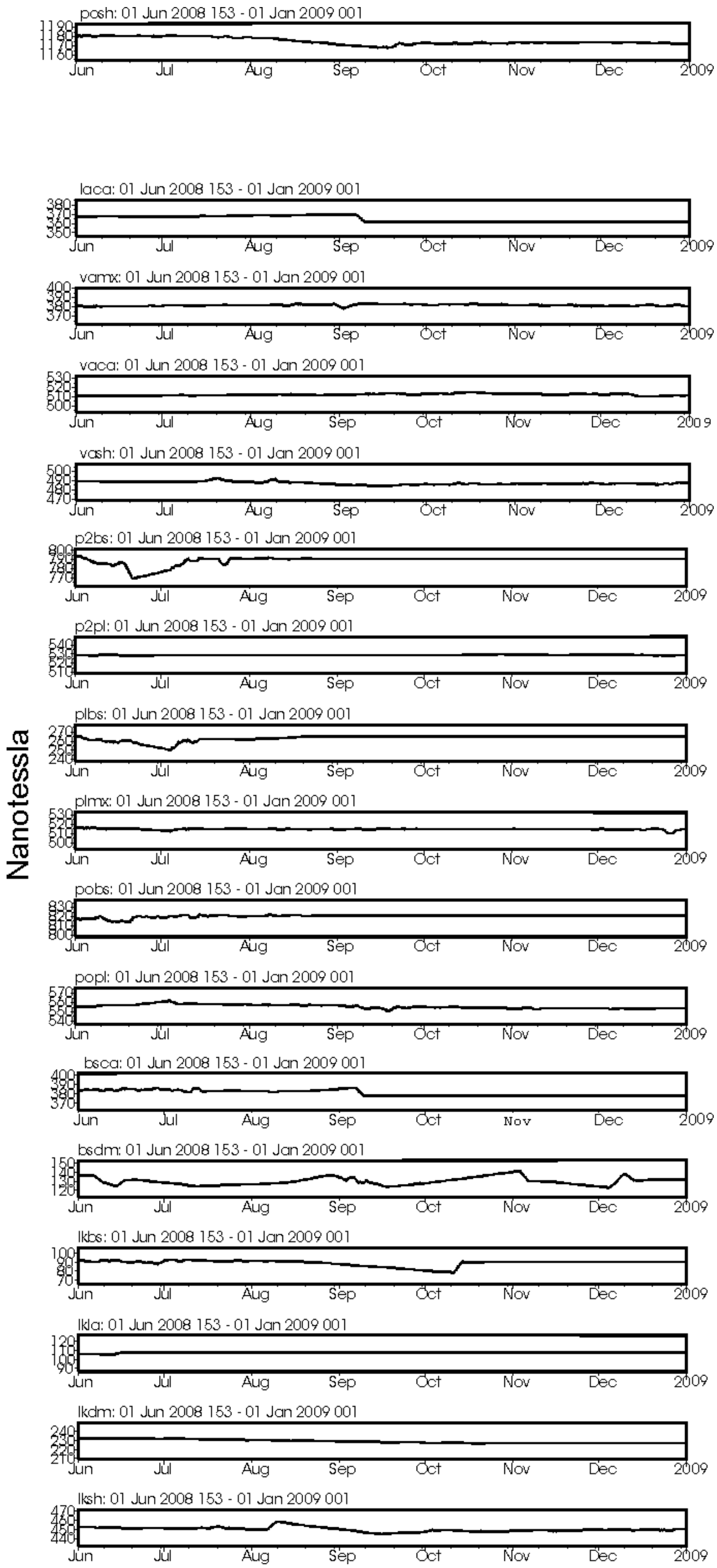

Figure M2. Differential magnetometer data for the stations shown in Figure M1: June-Dec 2008.

CO_2 STUDIES

HORSESHOE LAKE TREE-KILL AREA (Cindy Werner and Mike Doukas Cascades Volcano Observatory Vancouver, WA)

VEP maintains a CO_2 sensor network at Horseshoe Lake and also measures an array of points for CO_2 flux each year. Results of the 2008 data are summarized below.

Continuous CO_2 stations:

The GOES-telemetered carbon dioxide monitoring network in the Mammoth Lakes area continued to transmit data on soil gas carbon dioxide concentrations until August 2007 when the telemetry transmitters were removed. Data below represents the timeseries of data collected for the first year following the telemetry being removed. Station HS1 is located near the central portion of the Horseshoe Lake tree kill in an area of high CO_2 ground flux and has both a 0-100% sensor and a 0-50% CO_2 sensor (only data for 0-100% shown). Station HS2 is located in a lower flux area near the margin of the tree kill (not shown) and HS3 is at the edge of the tree-kill zone in the group campground area. Only one station is located away from Horseshoe Lake include SKI, located near the former Chair 19 in the Mammoth Mountain Ski Area (also not shown). At all sites, CO_2 collection chambers are buried in the soil. Air from these collection chambers is pumped to nearby carbon dioxide sensors housed in USFS structures or culverts. Local barometric pressure is also measured at HS1 using a Vaisala Pressure Transducer. Data were collected from the sensors every hour and logged onsite for downloading. Snow data were obtained from a U.S. Bureau of Reclamation monitoring station at Mammoth Pass

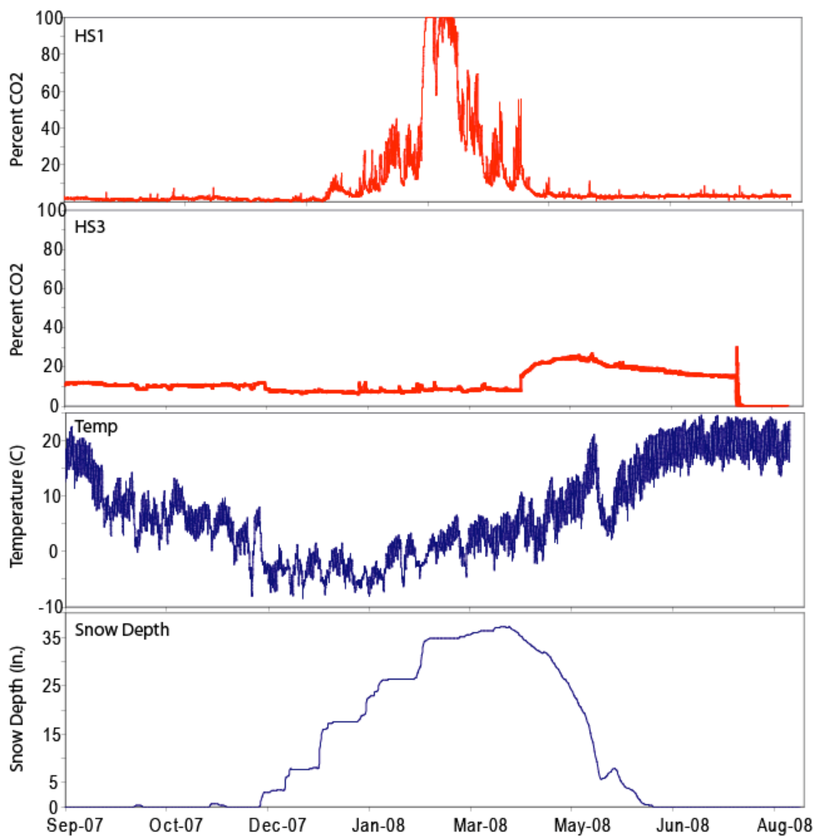

CO_2 data for 2007-2008 for are shown to the right along with air temperature and snow depth at Mammoth Pass. [**Note: Data not corrected for pressure and temperature.**] Station HS2 and SKI seemed to be not operating properly and are thus not shown.

The typical annual buildup of CO_2 at Horseshoe Lake as seen most years was visible in this year. As in previous years, HS1 sees the largest and earliest build-up; stations further from the main upflow of gas have a delayed increase (HS3 doesn't start increasing until April 2008).

CO_2 flux survey:

During the annual monitoring station servicing trip to Long Valley in August, CVO gas project personnel also conducted their annual soil CO_2 efflux survey at Horseshoe Lake. The results are shown below. The long term degassing rate average through 2005 had been about 100 tons of CO_2 per day at Horseshoe Lake. The rate measured in August 2008 was also near 100 t/d, slightly up from 2007 when emissions were on the order of 75 t/d.

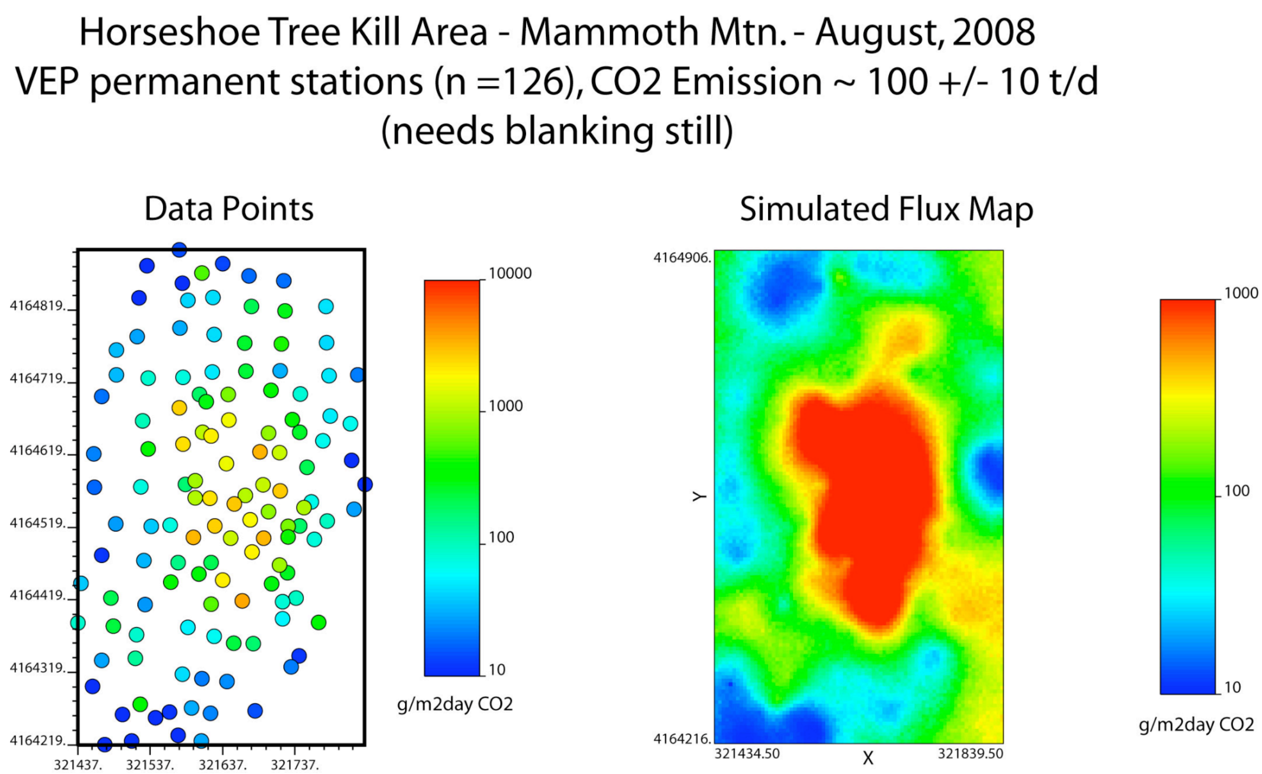

Carbon Dioxide Measurements at Mammoth Mountain (Christopher Farrar, Deborah Bergfeld, William Evans)

Background

Field surveys to measure and assess changes in carbon dioxide emissions from Mammoth Mountain were carried out during July and September 2008. Known CO_2 emission areas on Mammoth Mountain form a discontinuous ring around the south, west, and north sides of the mountain at altitudes between 2,700 and 3,000 meters. The largest areas emit CO_2

at ambient air temperatures diffusely from soils (sites HSL, RC, and CH-12 in fig cf-1). A few smaller areas of CO_2 emission, on the north and south flanks of the mountain, are associated with thermal ground and identifiable steam vents (MMF and SSF in fig cf-1). Measurements have been made annually at HSL for over a decade; more complete surveys that include HSL, RC, and CH12 have been made in annually since 2005 (table cf-1). Measurements in the two thermal areas have been less frequent. Prior to 2008, the last complete survey in SSF area was made in 1996. The chemical analysis of gas from a weak (60^{o} C) steam vent at SSF is compared to gas from MMF in table cf-2.

CO_2 emissions at over 700 stations were calculated from ground-based measurements of changes in CO_2 concentration in closed chambers (volume approximately 4 liters) over intervals from 1 to 3 minutes. CO_2 concentrations in the chambers were measured using infrared non-dispersive gas analyzers. Locations of measurement sites were determined with hand-held GPS receivers (generally precise to about 4-6 m). Total CO_2 flux from each area, expressed in tonnes per day (t/d), was estimated from grids of evenly spaced data produced by a Kriging interpolation routine run on the measured values.

Results

In July a survey focused on CO_2 emissions at HSL and SSF following a brief period of seismicity beneath the south flank of Mammoth Mountain. The CO_2 flux at HSL in July 2008 was estimated at 71 t/d and 46 t/d in September. The CO_2 flux of 7 t/d estimated for SSF in July was based on an incomplete survey of about 7 ha. In September the flux from an area of about 9.8 ha was estimated to be 12 t/d. The results of all the measurements made in 2008 are compared to similar measurements made in 1996 and 2005-2007 in table cf-1. Estimates of total CO_2 emission from the four sites on Mammoth Mountain based on data collected in 2008 are similar to the estimates made for 2005-2007. The total estimated for 2008, 95 t/d, is the highest for the four years but far lower than estimates from 1996. The differences in total emissions from the three largest areas (HSL, RC, CH12) between years 2005-2008 are not large (22 % of the mean of 74 t/d). Such differences may be related to variations in near surface conditions and may not signify changes in gas release from the source, several kilometers beneath the mountain. Variations in atmospheric conditions (pressure and wind), soil-moisture, the development of winter snowpack and melting, ground-water recharge and movement all can influence gas emissions from the soil. Also part of the differences in estimated emissions relate to slightly different boundaries used in the surveys between years.

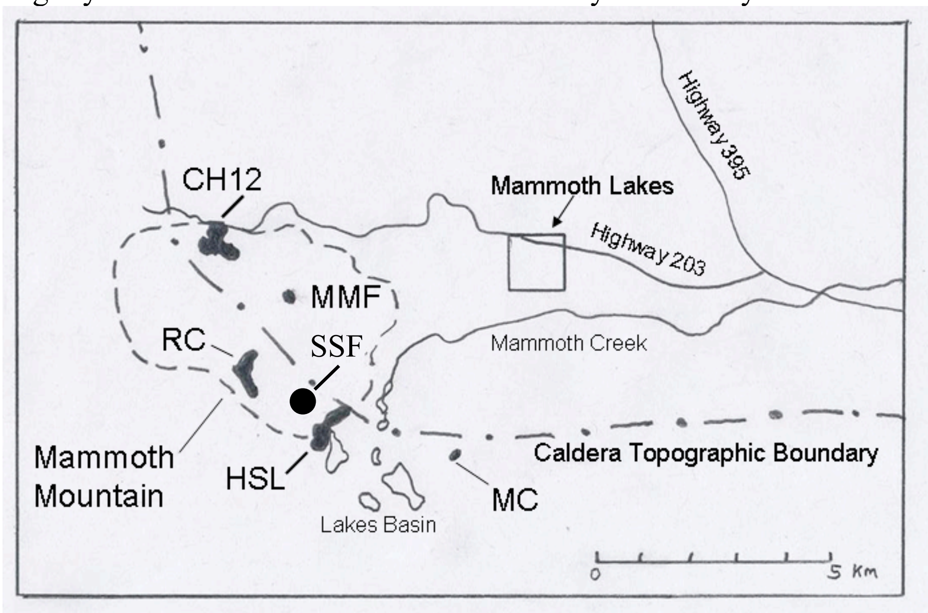

Figure cf-1. Locations of Carbon Dioxide Measurements

CF-1. Mammoth Mountain CO_2 Flux Summary

Location	Values in tonnes per day 1996	2005	2006	2007	2008
Horseshoe + Borrow Pit	134	40.1	22.2	27.2	[1] 46.0
Chair 12	48	17.4	13.0	24.6	17.0
Reds Creek	308	23.8	23.6	22.4	18.4
Southside	5	--	--	--	12.0
MMF	6	--	1.6	2.0	1.9
Total	501	81	60	76	95

1. Flux measured in July 2008 was 71.0

Table CF-2. Chemical Composition of Gas Samples

Normalized volume-percent

Site	Date	CO_2	N_2	O_2	Ar	H_2	He	H_2S	$^{3/4}He$
SSF	Aug. 2008	14.1	67.2	18.0	0.80	<0.0002	0.0007	<0.0005	--
MMF	Jul. 2008	98.4	1.5	0.2	0.0026	<.200	0.0023	--	5.55

DIFFUSE CO_2 STUDIES: MONO BASIN (Deborah Bergfeld, William Evans and Chris Farrar).

Background

Some of the most recent volcanism in the area around Long Valley produced explosion craters, lava flows, domes and cinder cones at locations in Mono Lake and along the Mono Craters chain, roughly 10 to 20 km north of the caldera. During 2007 we examined diffuse CO_2 emissions from 7 locations between the ~ 660 year old cinder cone on Paoha Island in Mono Lake and Devil's Punch Bowl along the southern section of the chain (Fig. 1). Of the sites visited in 2007 only North Coulee (NC) showed any evidence of anomalous diffuse CO_2 degassing.

North Coulee is composed primarily of a glassy rhyolite flow that is partially blanketed on the west by tephra deposits, there is no soil development and vegetative growth is sparse. The area lacks obvious clues such as chemical smells, stressed plants, or steaming ground that would otherwise identify diffuse degassing sites. There are a few localized sites with high flux and elevated soil temperatures that are evidenced by crusty surficial precipitates. Sites with bleached or reddish discolored rock show evidence of earlier hydrothermal activity. Most of these sites have normal soil temperatures and sometimes have anomalous CO_2 emissions, however our work has shown the altered sites are not always associated with a diffuse CO_2 flux.

When we completed the 2007 survey it was difficult to assess if we had discovered all anomalous degassing sites. We returned again in 2008 to repeat flux measurements over the 2007 grid and to investigate CO_2 emissions in areas containing altered rocks that were identified Google Earth images. A major thrust of the 2008 survey was to collect gas samples from high flux areas.

Methods

CO_2 concentration measurements were used to identify high flux areas. The measurements are made by driving a 1.5 m long hollow stainless steel probe into the ground and connecting the probe to a CO_2 analyzer. Gas is pumped from the tip of the probe to the detector and the CO_2 concentration is determined after allowing for the stored gas to be purged from the system. This set up is also used to collect gas samples by placing an evacuated sample bottle in line and collecting the gas after the system is purged.

CO_2 flux measurements are made using an accumulation chamber and a field-portable infrared CO_2 analyzer. The 2007 and 2008 studies included 224 and 174 flux measurements respectively, covering a portion of NC that is roughly 0.21 to 0.25 km^2 (Table 1). The average flux reported in units of grams of CO_2 per square meter per day ($g\ m^{-2}\ d^{-1}$) is determined from 1000 sequential Gaussian simulations of the measured flux data using the GSLIB program. To compare data from both years we omitted data from the 2007 locations that fall outside the footprint of the 2008 grid. Total CO_2 emissions in metric tonnes per day ($t\ d^{-1}$) are calculated by multiplying the average CO_2 flux by the grid area.

Highlights
At NC gas samples were collected at high flux sites from areas with both normal and elevated temperatures. Table 2 shows the composition of NC gas as well as samples from a large thermal spring on the south side of Mono Lake and from Mammoth Mountain fumarole (MMF) at Long Valley. The gas composition at NC is predominately air with excess CO_2 that ranges between 4 to 8%. A few samples show *slightly* elevated helium concentrations. In spite of the air-contamination carbon isotope analyses of the CO_2 indicate it is almost identical to the isotopic composition of deep CO_2 from Mammoth Mountain fumarole. Air-corrected $^3He/^4He$ ratios in two NC gas samples have R/R_c values of 5.1 and 6.6 and also indicate a deep source for the gas.

Flux maps from both years show similar results with a group of high flux sites clustered in the north part of the grid and a northerly-trending line of high flux sites along a steep ridge in the south. The average flux from both years was ~ 38 g m^{-2} d^{-1} and total CO_2 emissions were around 9 t d^{-1} (3 -16 t d^{-1}). It should be noted that given the lack of vegetation at NC there is no need to correct for biogenic CO_2 contributions and any diffuse CO_2 degassing is essentially anomalous. This supposition is supported by the fact that over 25% of the measurements from both years showed no flux.

This report corrects our earlier emissions estimate for North Coulee and shows a marked stability in the emissions rate. The carbon and helium isotope data confirm leakage of magmatically-derived gas that is largely diluted by a flux of atmospheric gas through the permeable tephra deposits. Although total CO_2 emissions at NC are much lower than what is observed at Long Valley the presence of a diffuse CO_2 flux is intriguing and it remains to be determined if CO_2 emissions are a remnant from earlier volcanism or are a sign of things yet to come. Given that NC and other nearby volcanic features are products of some of the most recent volcanism the region continued monitoring of the area is warranted.

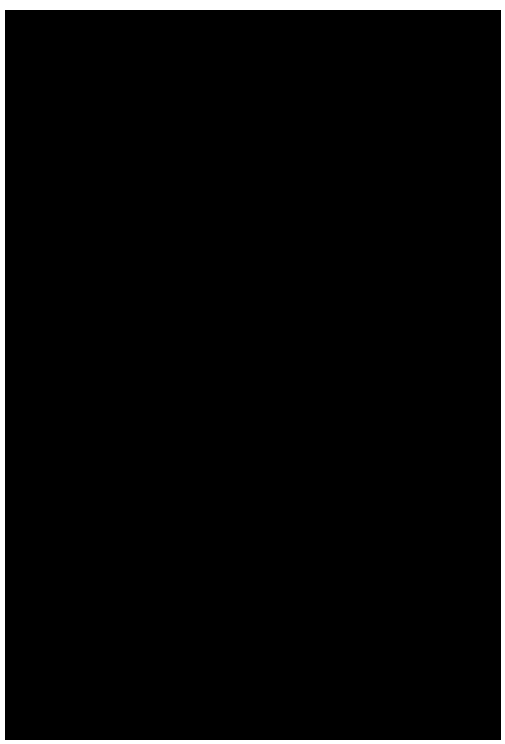

Figure 1. Map showing flux (black rectangles) sites along the Mono Craters chain and gas sample sites (x) from this study. Gas sample locations on North Coulee not shown. Panum Crater (PC), Navy Beach (NB), North Coulee (NC), Punch Bowl (PB), Mammoth Lakes (ML), Mammoth Mt. fumarole (MMF).

Table 1. Statistical results from sequential Gaussian simulations of the measured CO_2 flux.

Year	N	Max. Flux	Avg. Flux	Discharge ($t\,d^{-1}$)	Range ($t\,d^{-1}$)	Grid Area (km^2)
2007	208	2532	37.7	7.7	3 to 16	0.21
2008	174	1164	38.7	9.8	6 to 15	0.25

Table 2. Bulk chemistry and isotope results from gas collected at NC, Navy Beach soda spring on Mono Lake and Mammoth Mountain fumarole. Except for site 50 (10 cm) temperatures reported for NC sites were measured at 30 cm.

Sample #	Area	Date	T (C)	Depth (cm)	He	H_2	Ar	O_2	N_2	CH_4	CO_2	C_2H_6	H_2S	$(^{13}C-CO_2$	R_c/R_A
S 50	NC	06/27/08	23.7	nr	0.0009	<0.0002	0.8933	19.7	73.7	<0.0002	5.7	<0.0002	<0.0005	-4.9	--
S 73	NC	06/27/08	44.4	135	0.0010	<0.0002	0.8951	20.1	75.2	<0.0002	3.8	<0.0002	<0.0005	-4.9	--
S 68	NC	06/27/08	31.1	90	0.0006	<0.0002	0.8922	19.7	73.8	<0.0002	5.6	<0.0002	<0.0005	-5.0	--
GHF	NC	06/26/08	52.0	135	0.0006	<0.0002	0.8817	19.1	71.7	<0.0002	8.2	<0.0002	<0.0005	-4.9	6.6
Fum #2	NC	06/27/08	51.1	40	0.0005	<0.0002	0.8515	19.3	72.2	<0.0002	7.7	<0.0002	<0.0005	-4.9	5.1
Navy B. Soda	ML	06/25/08	32.6	na	0.0007	0.0007	0.0323	0.2	1.6	0.0023	98.3	<0.0002	<0.0005	-7.2	5.4
MMF	MM	06/27/08	nr	nr	0.0019	0.0211	0.0046	0.1	1.1	0.0027	98.7	<0.0002	0.0479	-4.5	5.6

HYDROLOGIC MONITORING (*Chris Farrar and Michelle Sneed: U.S. Geological Survey, Carnelian Bay and Sacramento, CA).*

Hydrologic data collected for the USGS Volcanic Hazards Program in this report include ground-water level data from four wells; stream flow, water temperature, and specific conductance from one site on Hot Creek; and estimated thermal water discharge in Hot Creek Gorge (figure H1). Additional data are available on the web at -- http://lvo.wr.usgs.gov/HydroStudies.html
or upon request – contact: *Chris Farrar at Carnelian Bay 530.546.0187.*

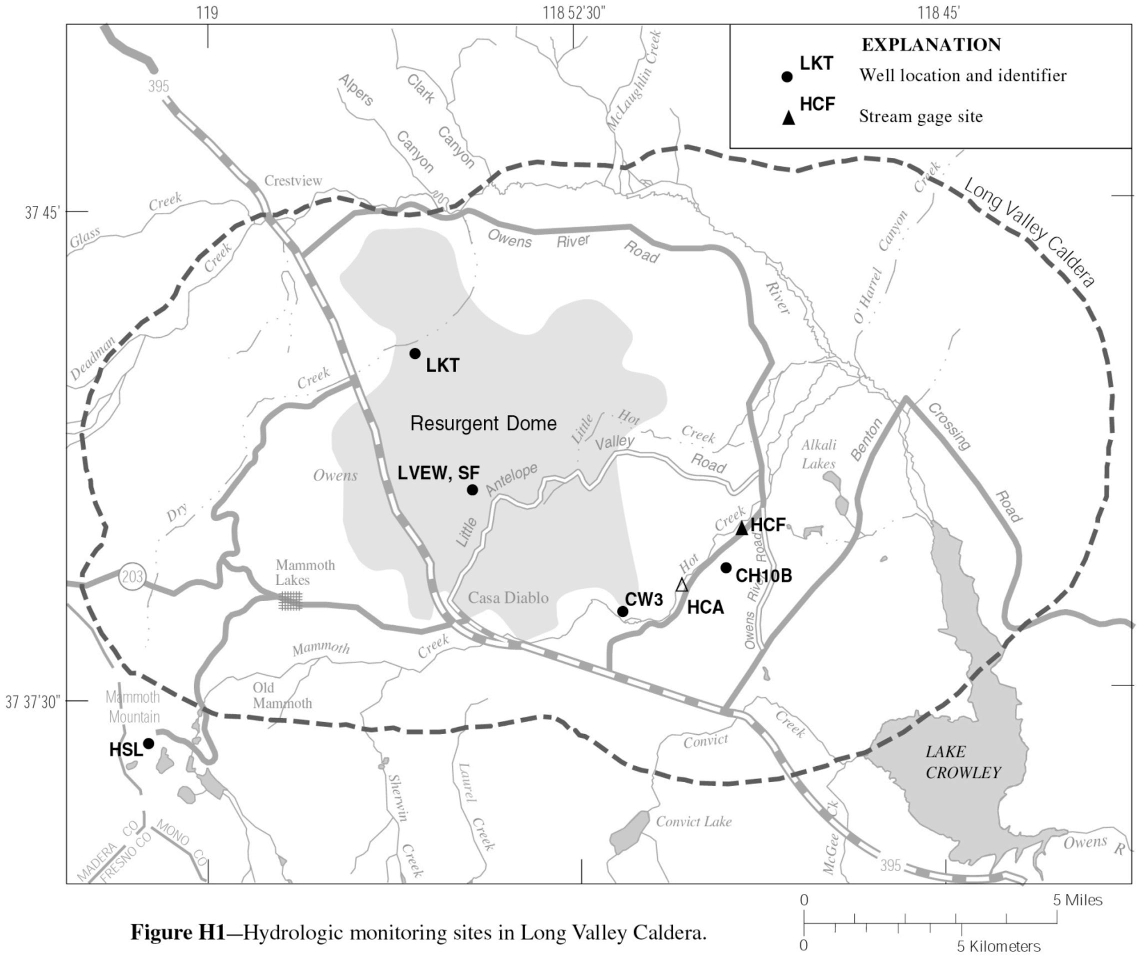

Figure H1—Hydrologic monitoring sites in Long Valley Caldera.

BACKGROUND

Ground-water levels in wells and the discharge of springs can change in response to strain in the Earth's crust. The network of wells and surface water sites provides hydrologic data that contributes to monitoring deformation and other changes caused from magmatic intrusions and earthquakes in Long Valley Caldera.

GROUND-WATER LEVEL MONITORING

Ground-water levels are measured continuously in four wells, LKT, LVEW, SF, and CH-10B (locations in figure H1), using pressure transducers that are either submerged below the water surface or placed above ground and sense back-pressure in a nitrogen-filled tube extending below the water surface. Barometric pressure is also measured at each site using pressure transducers. The data are recorded by on-site data loggers and telemetered on a three-hour transmit-cycle using the GOES satellite and receivers at Menlo Park and Sacramento. All sites are visited monthly to collect data from on-site recorders and to check instrument calibrations.

Data processing is done in the Sacramento Office. Records of barometric pressure are used in combination with the water-level records to determine aquifer properties from the observed water-level response to atmospheric loading and earth tides. The influences of barometric pressure changes and earth tides are removed from the water-level records. The result yields the filtered water-level record that may contain other hydraulic and crustal deformation signals. Filtered data for wells LKT and CH-10B are given in figures H2 and H3.

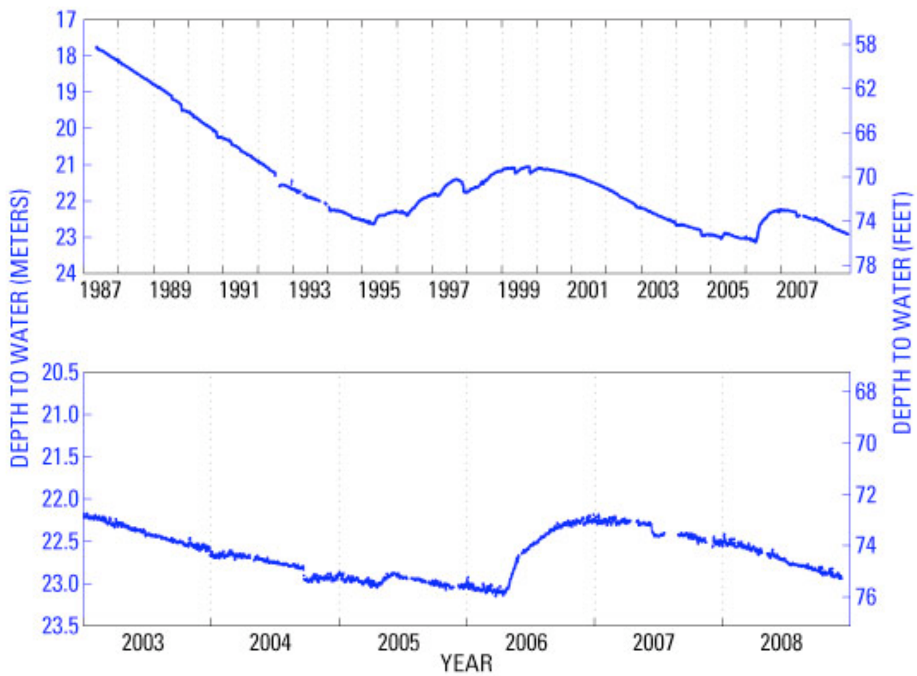

Figure H2. Hydrographs for well LKT, based on filtered daily mean values. The rise, beginning in mid-2006 is from a strong recharge pulse derived from the above average winter 2006 snow-pack. The decline in level that began in 2007 continued through 2008 because of minimal recharge in the northwest part of the caldera.

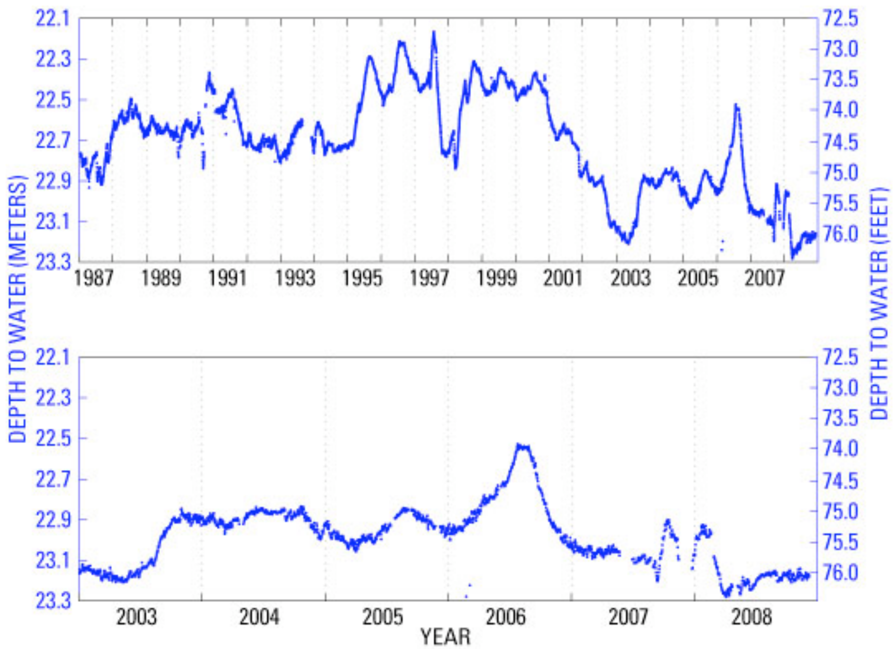

Figure H3. Hydrographs for well CH10B, based on filtered mean daily fluid levels. The large fluid level rise in mid-2006 is due to high recharge from above average precipitation during the winter of 2006. The fluid level oscillated about 0.2 m during the last half of 2007 and first part of 2008. In March, after reaching its lowest level in 21 years of observation, the level rose slightly. The oscillations in level are consistent with some of the shifting in locations of thermal spring discharge in Hot Creek Gorge.

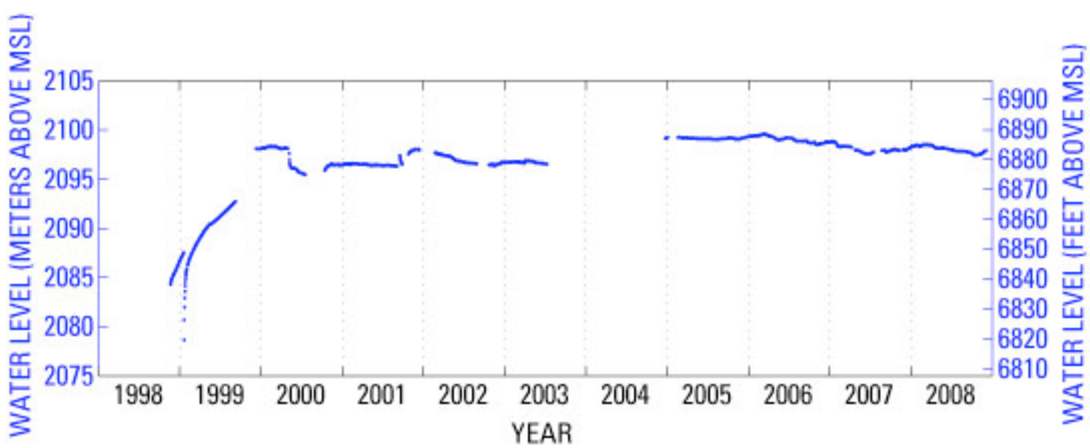

Figure H4. Unfiltered fluid levels in well LVEW.

The fluid level in well LVEW is controlled by the pressure in a fractured rock aquifer at a depth of about 3000 m below land surface and therefore is largely buffered against seasonal fluctuations. The early records from 1998-99 are strongly affected by well testing.

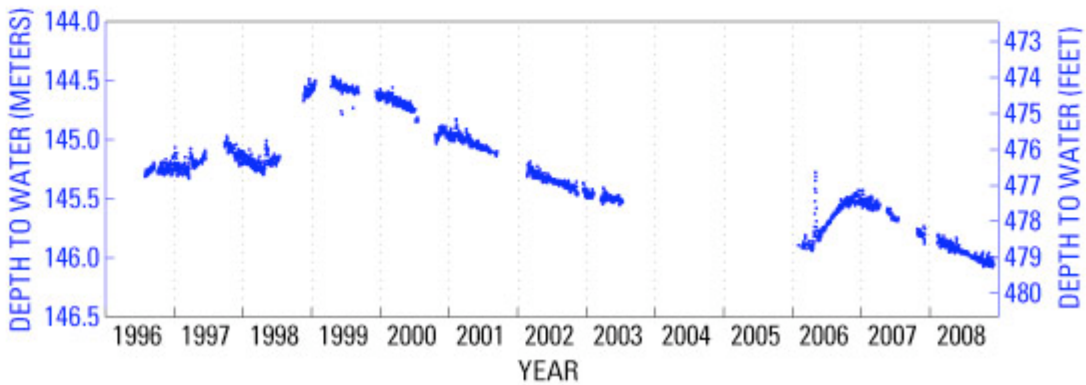

Figure H5. Unfiltered fluid levels in well SF, near LVEW.

The fluid level in well SF represents the hydraulic pressure in the upper 270 m of volcanic rock making up the resurgent dome. Fluid levels in SF respond to inter-annual patterns of precipitation and recharge. The fluid level dropped through 2007 and 2008, reaching its lowest level in 12 years of observation.

SURFACE WATER MONITORING

Site HCF is located downstream from the thermal springs in Hot Creek Gorge (figure H1). Stage, water temperature, and specific conductance (figure H6) are recorded every 15-minutes. The data are recorded by an on-site data logger and telemetered every three hours. Specific conductance is a measure of total dissolved ionized constituents. Water at HCF is a mixture of thermal water from springs along Hot Creek and non-thermal water from the Mammoth Creek basin. Changes in specific conductance are related to changes in the mixing ratio of thermal and non-thermal components of stream flow. Water temperatures change in response to ambient temperatures and the mixing ratio.

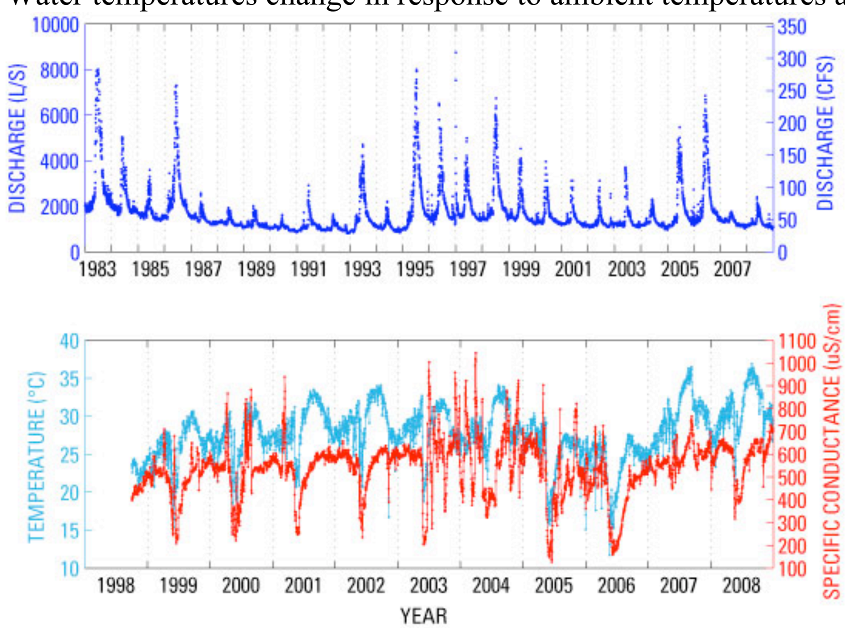

Figure H6. Discharge, water temperature, and specific conductance at Hot Creek Flume (HCF), based on daily mean data.

The effects of back to back winters with below average precipitation can be seen in the very small discharge peaks during spring runoff in 2007 and 2008. High water temperature and specific conductance throughout 2008 are the result of low discharge.

THERMAL WATER DISCHARGE ESTIMATE

Estimates of total thermal water discharge (figure H7) are computed from monthly measurements of discharge, and boron and chloride concentrations collected at a non-recording site (HCA) located upstream of the Hot Creek gorge thermal area and at site HCF downstream. The quantity of thermal water discharged to Hot Creek is known to vary in response to seasonal variations in precipitation, snow-melt, earthquakes, and other processes. It is believed that spring discharge may change in response to crustal strain.

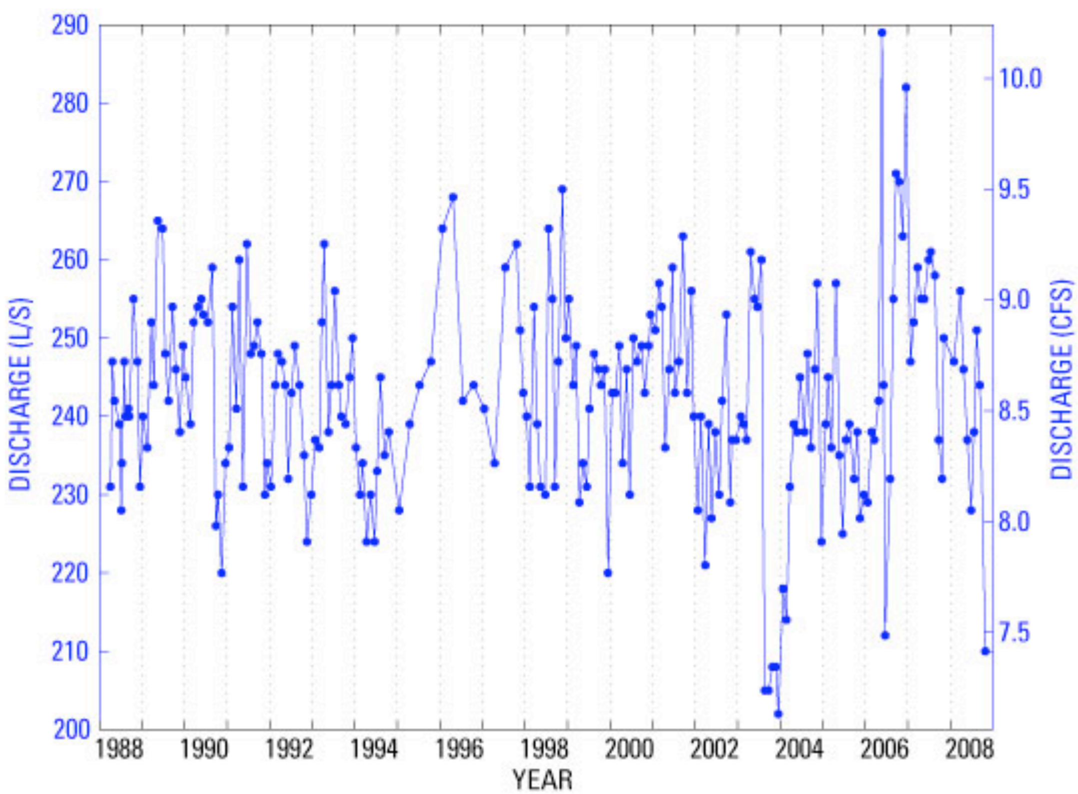

Figure H7. Estimated thermal water discharge for springs in Hot Creek Gorge.

Thermal springs in Hot Creek Gorge have continued to exhibit variability in discharge, temperatures, and vent locations throughout 2008. The vigorous fountaining-discharge from springs that began in May 2006 and continued into 2007 has been more subdued in 2008. The mean estimated total thermal water discharge of 240 L/s for 2008 is slightly less than the mean of 251 L/s for 2006 and 2007. Active spring vents along the banks of Hot Creek continued shifting locations in 2008. The U.S. Forest Service closure to swimming remains in effect because of the unpredictable behavior of the springs and areas of soil instability along the banks of Hot Creek.

REVIEW OF 2008

Relative quiescence has prevailed in Long Valley caldera and adjacent sections of eastern California from early 2000 through 2008. The resurgent dome, which essentially stopped inflating in early 1998 and showed minor subsidence (of about 1 cm) through 2001, was followed by a modest inflation episode through 2002. The gradual subsidence that began in 2003 appears to have flattened in early 2007, and the recent continuous GPS data show a slight hint of minor inflation beginning in mid-2008. The center of the resurgent dome remains some 75 cm higher than prior to the onset of unrest in 1980 (see Figure A1).

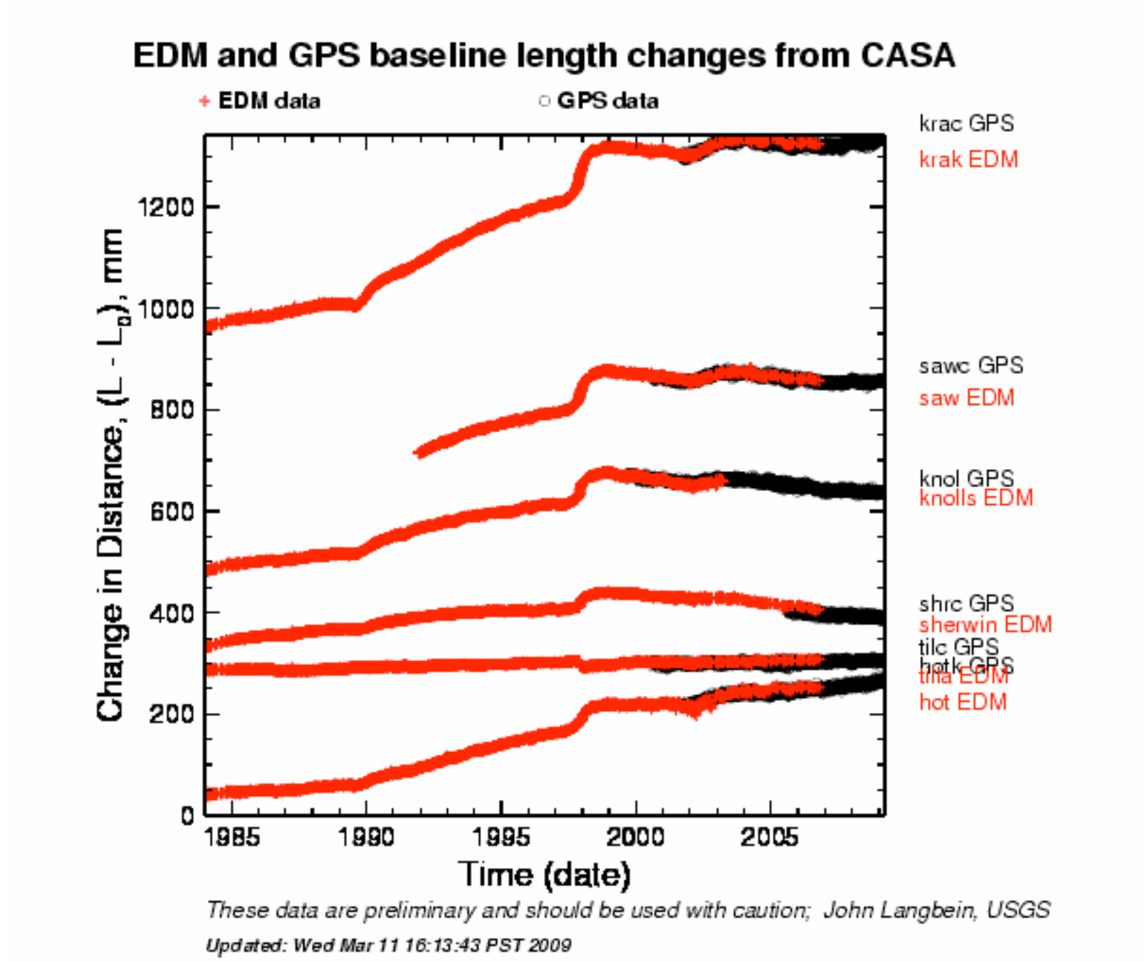

Figure A1. History of extension across the resurgent dome from mid-1984 through the end of 2008 based on frequent line-length measurements using the 2-color EDM (red) and differential continuous GPS measurements (black). Line-length extension turns out to be a good proxy of uplift of the central part of the resurgent dome.

Earthquake activity within the caldera during 2008 remained low with no earthquakes exceeding magnitude M=2.0 (Figures A2 and A4). Mammoth Mountain activity, however, increased somewhat with swarms of small earthquakes on April 7, June 29, July 15, August 10, October 15, and December 14. Each of these swarms included one or more "spasmodic bursts", or rapid-fire sequences of small earthquakes with overlapping seismic waves commonly persisting for periods of several minutes. The Mammoth Mountain activity included five earthquakes with magnitudes M=2.0 or larger, the largest a M=2.5 event during a swarm on October 15 (Figure A5). Seismic activity throughout the greater Long Valley region included six earthquakes with magnitudes greater than M = 3.0, the largest of which was a M = 3.9 event on June 29 located 2 miles east of Convict Lake (Figure A2 and A3). This earthquake produced perceptible shaking in Mammoth Lakes and vicinity.

As in the past, most of the regional earthquake activity was concentrated in the Sierra Nevada south of the caldera, the corridor between Round Valley and Bishop, the Chalfant Valley, and the Abobe Hill east of Mono Lake. This activity included seven earthquakes with magnitudes of M=3.0 or greater, the largest being a M=3.9 event on June 29 located two miles east of Convict Lake. This earthquake produced perceptible shaking throughout the Mammoth Lakes area.

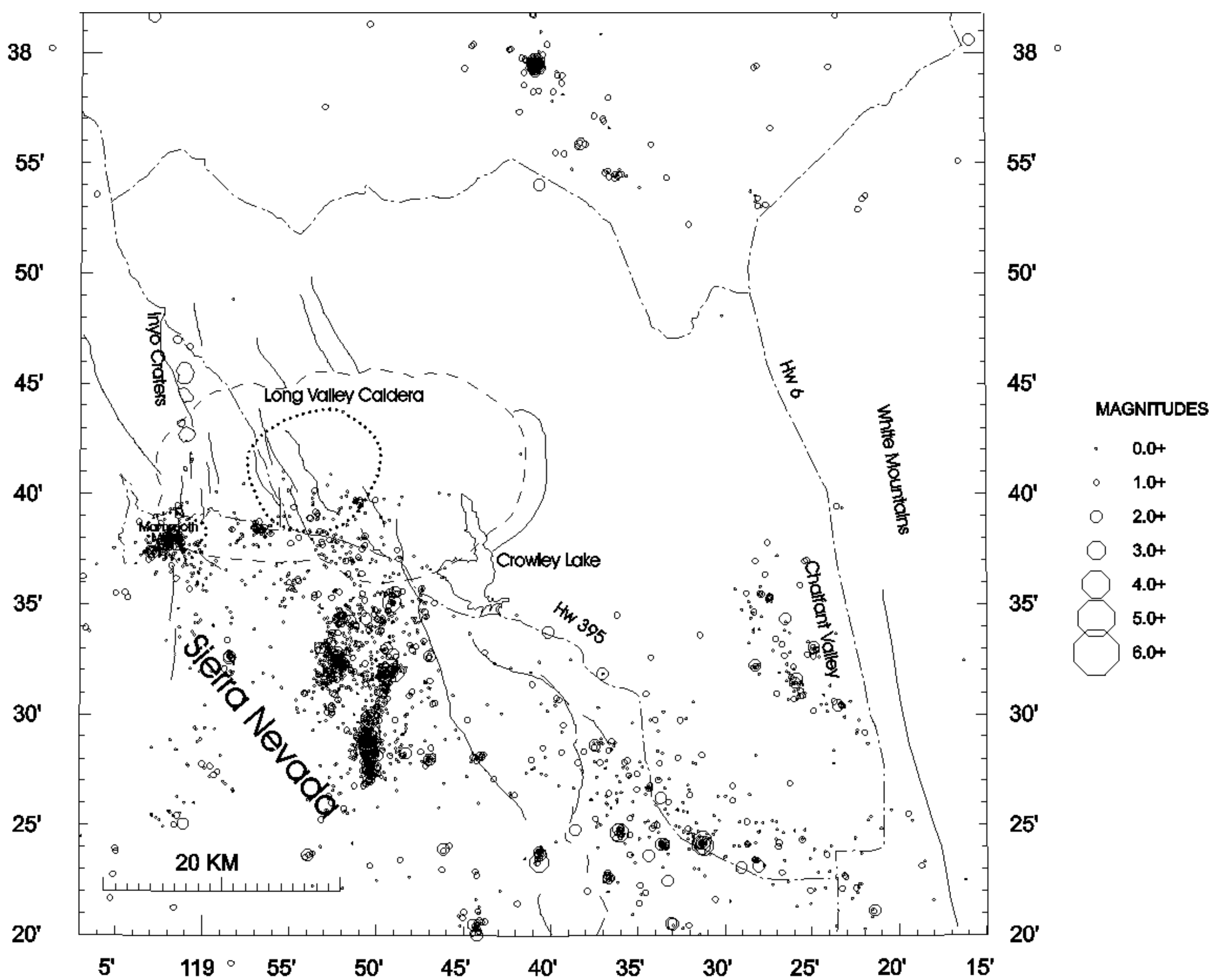

Figure A2: All earthquake epicenters in the Long Valley region for 2008

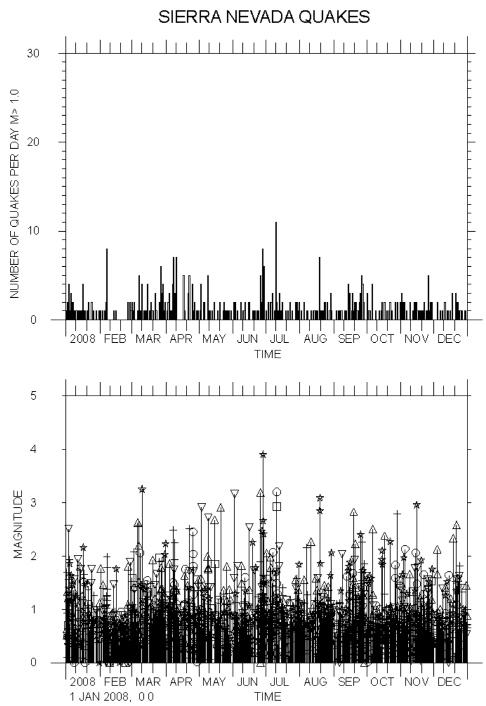

Figure A3: Temporal occurrence of earthquakes in geographic subregions of the area shown on figure A2. Top: number of >M1 events per day. Bottom: event magnitudes proportional to line length with focal depth indicated by symbol at top of line.

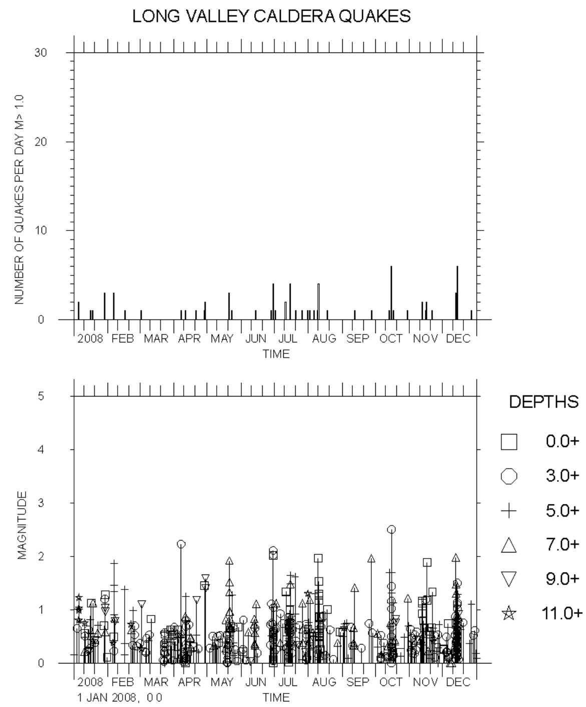

Figure A4: Temporal occurrence of earthquakes in geographic subregions of the area shown on figure A2. Top: number of >M1 events per day. Bottom: event magnitudes proportional to line length with focal depth indicated by symbol at top of line.

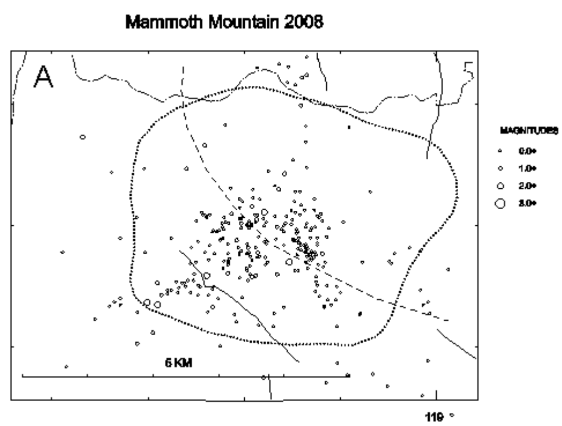

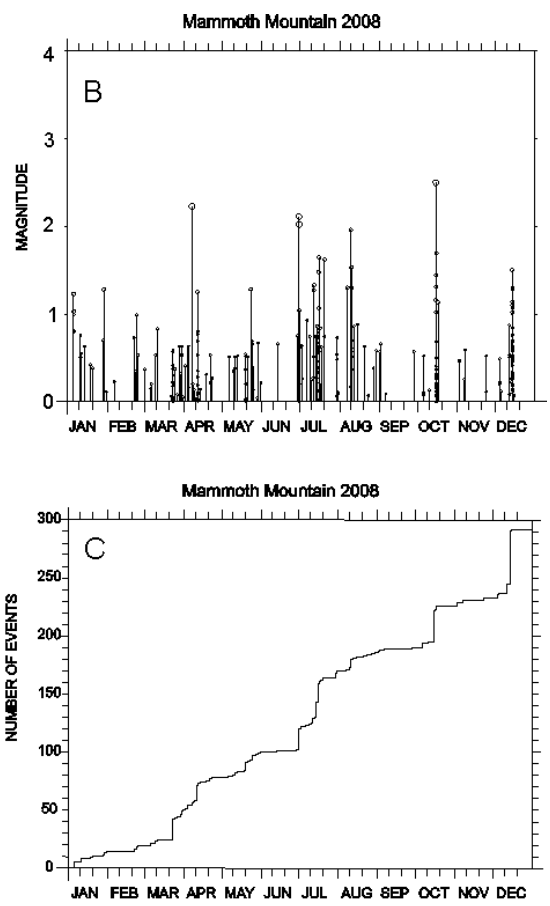

Figure A5: Mammoth Mountain seismicity for 2008.

A) Map of earthquake epicenters scaled by magnitude. Dotted line is Mammoth Mountain outline, dashed line is the southwest margin of Long Valley caldera beneath Mammoth Mountain, solid lines are mapped faults.

B) Earthquake magnitudes with time.

C) Cumulative number of earthquakes with time.

Carbon dioxide emissions around Mammoth Mountain continue to fluctuate with measurement in the Horseshoe Lake area varying between 50 and 100 tons/day. Repeat occupations of CO_2 flux sites on the Mono Craters reveal that vents on North Coulee continue to produce about 9 tons/day with an isotopic composition essentially the same as that for Mammoth Mountain.

Hydrological monitoring reveals no evidence for deep-seated changes in the hydrothermal system within the caldera during 2008.